crystals

MDPI

Article

About the Role of Fluorine-Bearing Apatite in the Formation of Oxalate Kidney Stones

Anatolii V. Korneev, Olga V. Frank-Kamenetskaya and Alina R. Izatulina *

Crystallography Department, Institute of Earth Sciences, St. Petersburg State University, 7/9, University emb., 199034 St. Petersburg, Russia; a_v_korneev@list.ru (A.V.K.); ofrank-kam@mail.ru (O.V.F.-K.)

* Correspondence: alina.izatulina@mail.ru; Tel.: +7-911-770-3824

Received: 27 April 2020; Accepted: 5 June 2020; Published: 6 June 2020

Abstract: Using electron microprobe analysis, 17 kidney stones containing apatite were studied. According to the results of the research, it was found that the apatite of all the oxalate kidney stones contained fluorine, while in the apatite of the phosphate kidney stones, fluorine was present in trace amounts or absent. Direct correlation between the amount of oxalate mineral phases and the fluorine content was observed. Ionic substitutions in the apatite of kidney stones have a multidirectional effect on the unit cell parameters. The fluorine content increases with the increase of *a* unit cell parameter, which is probably associated with a simultaneous increase in the amount of H_2O in the structure of apatite. The results of thermodynamic modeling show that fluorapatite is stable at lower pH values than hydroxylapatite, and therefore can be a precursor of calcium oxalates crystallization.

Keywords: biominerals; kidney stones; pathogen crystallization; X-ray diffraction; calcium oxalates; fluorine; fluorapatite; apatite; nucleation

1. Introduction

Urolithiasis disease has been known since ancient times [1], and it is widespread nowadays. The lifetime risk of kidney stone formation is about 10%–15% in the developed countries, but can be as high as 25% [2]. Despite the fact that the most common phases of kidney stones are calcium oxalates [2,3], calcium and magnesium phosphates are also quite common phases and play an important role in stones' formation. Apatite is one of main mineral components of human tissues and occurs (often in trace amounts) in almost all urinary stones as well [4]. According to the powder X-ray diffraction (PXRD) analysis of the kidney stones from our collection, which consist of about 2000 samples removed from residents of the St. Petersburg and Leningrad region (Russian Federation), about 74.5% of the samples consisted of calcium oxalates. Moreover, most of oxalate stones contained apatite as well, and apatite is also the main component of phosphate stones (64.7%). The prevalence of apatite in urinary stones was also confirmed in a number of works from other researchers. For example, Otnes, 1983 [5], detected apatite in 164 stones out of 175. Most stones have a nucleus of apatite, which suggests that apatite is the first mineral phase that crystallizes in human urea [6,7]. In 1937, Randall [8] described calcium-containing plaques in the renal papillae and hypothesized that the formation of kidney stones begins with these plaques due to the formation of primary tissue lesions, which are a subepithelial form of hydroxylapatite [9–11]. Stone formation occurs in urine in two stages: 1. the core formation; and 2. the formation of an aggregate from this core. The first step gives an idea of the thermodynamics of nucleation and growth, while the second stage is determined by the kinetics of the process. The formation of oxalates on the apatite core does not contradict thermodynamic calculations [12], according to which the probability of the formation of calcium oxalates is small compared to phosphates. A number of works [7,13,14] are devoted to the formation of oxalate stones

on calcium phosphate nuclei. Thus, Xie et al. [14] showed that stones composed of monohydrate calcium oxalate whewellite are aggregates around the calcium phosphate core.

The apatite of kidney stones is not well crystallized, which complicates its study by PXRD methods. Moreover, the complexity of the composition of physiological fluid (urine) leads to variations of the unit cell parameters of kidney stone apatite compared with stoichiometric apatite, which can be attributed to the substitutions in all crystallographic sites [15,16]. In particular, variations of the unit cell parameters can be caused by substitutions of OH^- ions by F^- ions in the channels of the apatite crystal structure.

The aim of this work was to clarify fluorine contribution in kidney stone formation and their chemical composition.

2. Materials and Methods

Seventeen samples of urinary stones (10 samples from male and 7 from female patients, aged from 22 to 67) of St. Petersburg and Leningrad region (Russian Federation) citizens were taken for further investigation using the following set of methods.

PXRD was performed using Rigaku Miniflex II, Rigaku IV Ultima or Bruker D2 Phaser (CuKα radiation, $2\theta = 5°–60°$) diffractometers to study the qualitative and quantitative composition of the kidney stones. Phases were identified using the ICDD PDF-2 Database (release 2016; Newtown Square, PA, USA). The unit cell parameters of apatite were refined by the Pawley and Rietveld methods using the TOPAS 4.2 software [17].

Scanning electron microscopy (SEM) was used to obtain images of the urinary stones by the means of a Hitachi S-3400N (operated at 20 kV, 1 nA probe current, working distance 10 mm). Energy-dispersive X-ray spectroscopy analysis (EDX) was performed in order to determine the fluorine content in the apatite using carbon-coated polished thick sections of kidney stones using an Oxford Instruments X-Max 20 spectrometer. SrF_2 and BaF_2 were used as a standards, determination error is ±0.2 wt%.

Thermodynamic calculations of the fluorapatite and hydroxylapatite stability field were performed to estimate the probability of the F-bearing apatite participation in the formation of kidney stones. An algorithm similar to that presented in [12] was used. The following thermodynamic data (Table 1) were used for the calculations. Thermodynamic constants were not corrected for the temperature of the human body and activity coefficients were set to unity.

Table 1. Thermodynamic data used for the calculations.

Composition/Ion	$\Delta_f G^\circ_{298}$, kJ/mol	Reference
Fluorapatite $Ca_5(PO_4)_3F$	−6455.778	[18]
hydroxylapatite $Ca_5(PO_4)_3OH$	−6286.093	[18]
Ca^{2+}	−552.706	[19]
$Ca(OH)^+$	−716.970	
$Ca(OH)_2$	−897.008	
PO_4^{3-}	−1018.804	
HPO_4^{2-}	−1089.263	
$H_2PO_4^-$	−1130.391	
H_3PO_4	−1142.650	
OH^-	−157.293	
F^-	−279.993	
HF	−293.825	
H_2O	−237.178	

The expression for conditional solubility constant is:

$$SP_{cond} = \frac{SP}{\alpha^a_{M^{m+}} \alpha^b_{A1^{n-}} \alpha^c_{A2^{k-}}} = C^a_M C^b_{A1} C^c_{A2},$$

where α are the molar fraction of ions. The chemical equilibrium between hydroxylapatite and the solution can be described by its surface with the equation:

$$\log_{10}\left[Ca^{2+}\right] = \frac{1}{5}(SP - 5\alpha_{Ca^{2+}} - 3\alpha_{PO_4{}^{3-}} - \alpha_{OH^-}) - \frac{3}{5}\log_{10}\left[PO_4{}^{3-}\right] - \frac{1}{5}\log_{10}[OH^-].$$

The equation for fluorapatite includes [F$^-$] instead of [OH$^-$]. The concentration of fluorine in human urine ranges from 0.2 to 2 mg/L [20–22] and was taken as 1 mg/L for this study.

Molar fractions α can be calculated as $\alpha_{M^{m+}} = \frac{[M^{m+}]}{c_{M^{m+}}}$ and $\alpha_{A^{n-}} = \frac{[A^{n-}]}{c_{A^{n-}}}$. Therefore:

$$\alpha_{Ca^{2+}} = \frac{[Ca^{2+}]}{c_{Ca^{2+}}} = \frac{[Ca^{2+}]}{[Ca^{2+}] + [Ca(OH)^+] + [Ca(OH)_2]} = \frac{1}{1 + \frac{10^{(pH-14)}}{K_{m2}} + \frac{10^{2(pH-14)}}{K_{m1}K_{m2}}}$$

$$\alpha_{PO_4{}^{3-}} = \frac{[PO_4{}^{3-}]}{c_{PO_4{}^{3-}}} = \frac{[PO_4{}^{3-}]}{[PO_4{}^{3-}] + [HPO_4{}^{2-}] + [H_2PO_4{}^{2-}] + [H_3PO_4]} = \frac{1}{1 + \frac{10^{-pH}}{K_{a3}} + \frac{10^{-2pH}}{K_{a2}K_{a3}} + \frac{10^{-3pH}}{K_{a1}K_{a2}K_{a3}}}$$

$$\alpha_{OH^-} = \frac{[OH^-]}{c_{OH^-}} = \frac{[OH^-]}{[OH^-] + [H_2O]} = \frac{1}{1 + \frac{10^{-pH}}{K_{H_2O}}}$$

$$\alpha_{F^-} = \frac{[F^-]}{c_{F^-}} = \frac{[F^-]}{[F^-] + [HF]} = \frac{1}{1 + \frac{10^{-pH}}{K_F}}$$

K_{m1}, K_{m2} are stepwise constants of dissociation for $Ca(OH)_2$. K_{a1}, K_{a2}, K_{a3} are stepwise constants of dissociation for H_3PO_4. K_F is the constant of dissociation for HF. K_{H2O} is the constant of dissociation for water.

The constants and solubility products were calculated using the equation:

$$\Delta_r G^0 = -RT * \ln(K) = RT * \ln(SP).$$

3. Results

3.1. X-ray Diffraction

According to the PXRD analyses, all the stones studied herein contained apatite (Table 2, Figure 1). The portion of apatite varied from 9.6% to 94.6%. All the stones could be divided into two groups: 12 oxalate-bearing samples (contained calcium oxalates—calcium oxalate monohydrate (whewellite $CaC_2O_4{\cdot}H_2O$) and calcium oxalate dihydrate (weddellite $CaC_2O_4{\cdot}(2.5 - x)H_2O$) and five pure phosphate samples (contained only struvite $NH_4Mg(PO_4)^*6H_2O$ and apatite $Ca_5(PO4)_3(OH,F)$). One oxalate-bearing stone among the studied stones contained struvite, and one of the oxalate-bearing stones contained anhydrous uric acid (mineral uricite $C_5H_4N_4O_3$ [23]).

Table 2. Mineral composition of the studied kidney stones.

Sample	Whewellite, %	Weddellite, %	Struvite, %	Apatite, %
1	0.0	0.0	23.8	76.2
2	7.0	64.0	0.0	29.0
3	46.8	7.9	0.0	45.3

Table 2. *Cont.*

Sample	Whewellite, %	Weddellite, %	Struvite, %	Apatite, %
4	80.8	9.6	0.0	9.6
5	23.2	45.5	0.0	31.3
6	11.8	1.0	5.4	81.8
7	76.6	2.9	0.0	20.5
8	5.3	57.5	0.0	37.2
9	2.3	16.6	0.0	81.1
10	63.4	5.3	0.0	31.3
11	49.2	5.7	0.0	45.1
12	0.0	0.0	54.7	45.3
13	48.4	41.9	0.0	9.7
14 *	0.0	6.0	0.0	77.0
15	0.0	0.0	50.0	50.0
16	0.0	0.0	5.4	94.6
17	0.0	0.0	55.0	45.0

* 17% uricite

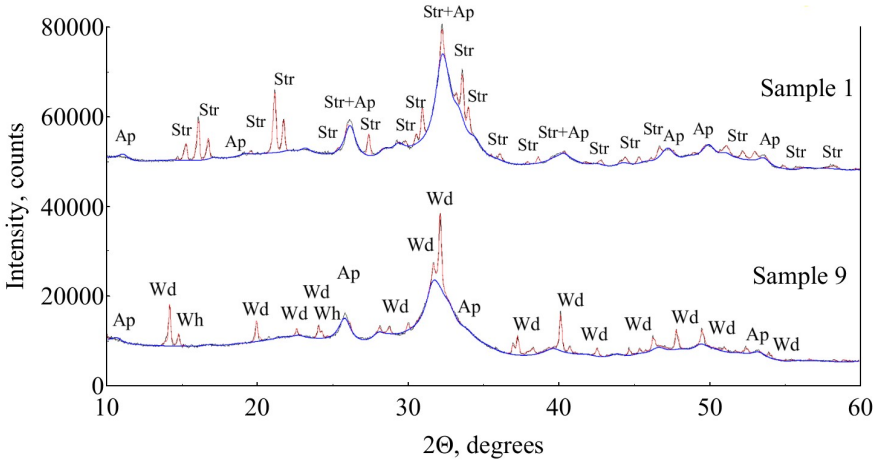

Figure 1. XRD patterns of the pure phosphate (sample 1) and oxalate-bearing (sample 9) kidney stones (red lines). The blue lines indicate the contribution of apatite in each XRD pattern (calculated by the Pawley method). Wh—whewellite, Wd—weddellite, Ap—apatite, Str—struvite.

Apatite has broad peaks in the XRD patterns (Figure 1, Sample 1) due to the low crystallinity degree (size of the crystallites ranges from 3 to 50 nm), which complicates its study.

Unit cell parameters of apatite from the studied urinary stones (Table 3) vary in the wide range of 9.365(2)–9.437(3) Å for *a* and 6.854(2)–6.882(2) Å for *c*.

Table 3. Unit cell parameters of apatite from the studied urinary stones *.

Sample	a, Å	c, Å	Crystallite Size, nm
2	9.437	6.872	10(1)
3	9.399	6.854	20(3)
4	9.409	6.882	19(4)
5	9.432	6.871	11(1)
6	9.415	6.878	8(1)
7	9.402	6.865	50(30)
8	9.429	6.874	10(1)

Table 3. *Cont.*

Sample	a, Å	c, Å	Crystallite Size, nm
9	9.425	6.854	8(1)
10	9.415	6.874	21(5)
11	9.397	6.861	34(11)
13	9.411	6.880	13(5)
14	9.427	6.875	8(1)
1	9.393	6.878	7(1)
12	9.408	6.870	8(1)
15	9.365	6.878	7(1)
16	9.417	8.867	3(1)
17	9.395	6.869	9(1)

* Estimated standard deviations of values do not exceed 0.004 Å

3.2. SEM and EDX

It is known that kidney stones are divided into two types according to their structural and textural features: stones of crystallization and agglomeration types [4]. According to SEM studies, the studied oxalate kidney stones, which consist of whewellite and weddellite, are characterized mainly by crystallization structures (Figures 2a, 3 and 4), with spherulitic zonal structures (Figure 4), and dendritic structures composed of individual weddellite crystals (Figures 2a and 3). Phosphate kidney stones studied herein are related to the agglomeration type of structures [24]. The structure of phosphate uroliths is fine grained or, more often, cryptocrystalline, which indicates the formation of stone by the agglomeration of microcrystalline or amorphous material (Figure 2b,c and Figure 5). Concentric zoning is characteristic for most urinary stones (Figures 2, 4 and 5). Minerals form subsequent layers clearly visible in SEM images. Phosphate minerals do not form distinctive crystals, while oxalates form bipyramidal crystals with sharp edges (weddellite) or do not form visible edges (whewellite). In addition, kidney stones can be characterized by the different contents of organic matter.

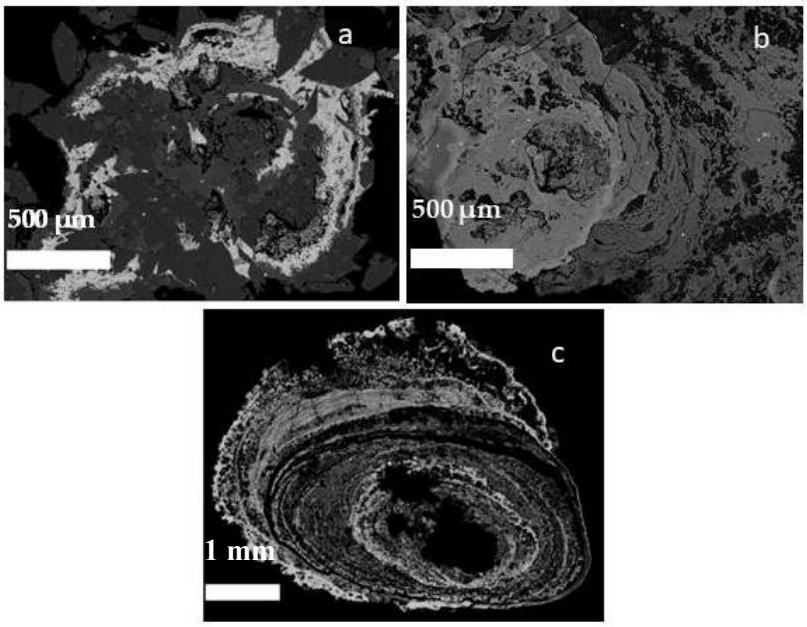

Figure 2. SEM BSE images of the oxalate-bearing stones, Sample 5 (**a**) and the pure phosphate stones, Sample 1 (**b**) and Sample 17 (**c**).

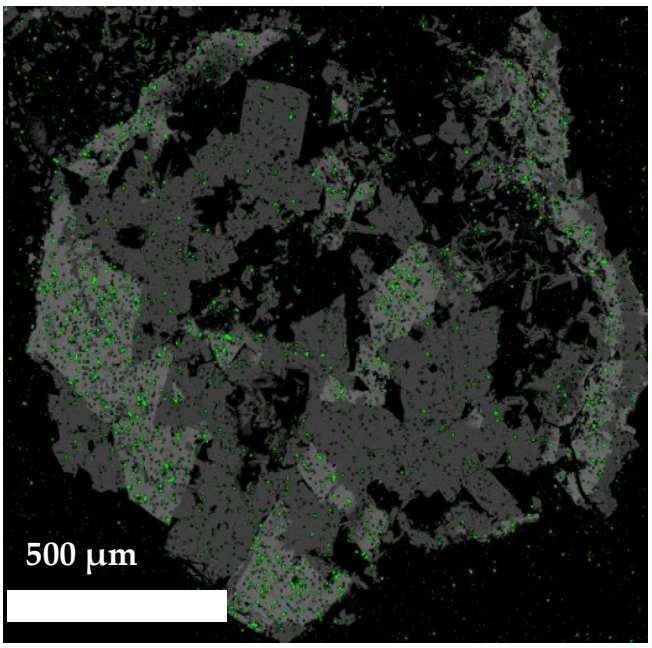

Figure 3. Fluorine distribution within the oxalate-bearing stone, Sample 10. BSE image.

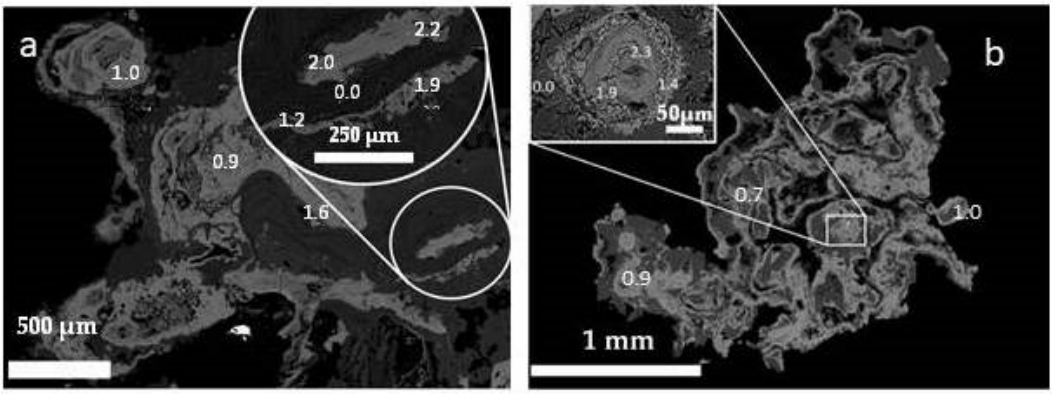

Figure 4. Examples of fluorine distribution in the oxalate-bearing stones, Samples 1703 (**a**) and 1384 (**b**). BSE images.

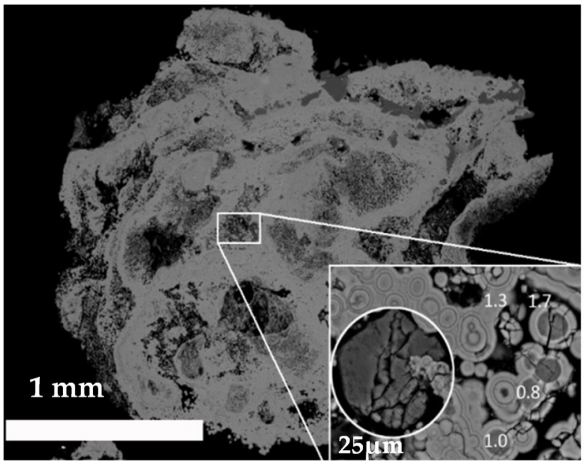

Figure 5. Globular apatite with a high F concentration in the center of the oxalate-bearing kidney stone, Sample 14. BSE image.

The results of the EDX studies show the fluorine concentrates in apatite and not in calcium oxalates (Figure 3). The average fluorine concentrations varied from 0 to 0.59 in the pure phosphate stones and from 0.61 to 1.84 wt% in the oxalate-bearing stones (Table 4).

Table 4. Average fluorine concentrations in the studied urinary stones.

Sample	F, wt%
Stones with calcium oxalates (oxalate-bearing)	
2	1.14
3	1.51
4	1.84
5	1.82
6	0.79
7	1.07
8	1.20
9	0.61
10	1.22
11	1.13
13	1.77
14	1.29
Stones with no calcium oxalate (pure phosphate)	
1	0.12
12	0.37
15	0.59
16	0.56
17	0.00

Sample 14 (Figure 5) attracts special attention due to the low content of calcium oxalates (6% of weddellite) and with an average concentration of fluorine (1.35 wt%), in which fluorapatite is represented by globules with a size less than 10 μm that are associated with weddellite. At the same time, the central part of the stone consists entirely of apatite, which, apparently, indicates a possible increase in pH and changes in crystallization conditions.

Fluorine is spread irregularly and its content varied from 0 to 2.4 wt%. The fluorine concentration in the apatite in the central part of the oxalate-bearing stones was generally higher than at the periphery (Figure 4).

3.3. Thermodynamic Modelling

The results of thermodynamic calculations (Figure 6) which were performed using the Maple 15 software have shown that the solubility of fluorapatite is lower than the solubility of hydroxylapatite. This demonstrates the higher stability of the fluorapatite in comparison with hydroxylapatite within the studied ranges of pH and the concentrations of Ca^{2+} and $(PO_4)^{3-}$ ions.

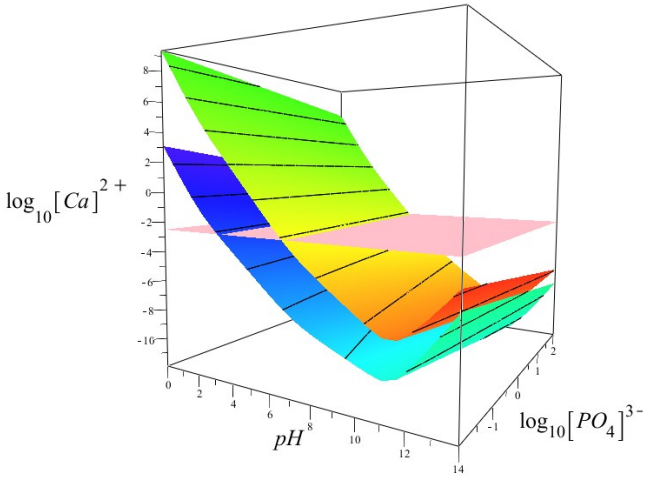

Figure 6. Solubility diagrams for the fluorapatite (lower) and hydroxylapatite (upper); the pink plane shows the average concentration of Ca^{2+} ions in the physiological solution.

4. Discussion

4.1. Variation of Apatite Unit Cell Parameters

The range of apatite unit cells parameters from the studied kidney stones (Table 3) was in good agreement with the previously estimated values (a = 9.395(4)–9.457(4) Å, c = 6.849(3)–6.885(4) Å (Figure 7) [15], revealing the diversity of their chemical composition and the significant variations in its formation conditions. It is known that the apatite of urinary stones is a Ca-deficient H_2O-bearing carbonated hydroxylapatite of the B-type [15,25]. The increase of the a unit cell parameter comparing to the stoichiometric hydroxylapatite (a = 9.418, c = 6.884 Å JCPDS № 9-432) mainly occurs due to the substitution of OH^- ions by H_2O molecules in the channels of the structure, whereas the reduction of the parameter occurs due to the $(CO_3)^{2-}$ for $(PO_4)^{3-}$ ion substitution and the OH^- for F^- ions. The reduction of the c unit cell parameter lower than that for the stoichiometric hydroxylapatite indicates that the effect of the vacancies at the Ca sites was significantly larger than in the $(CO_3)^{2-}$ for $(PO_4)^{3-}$ substitution.

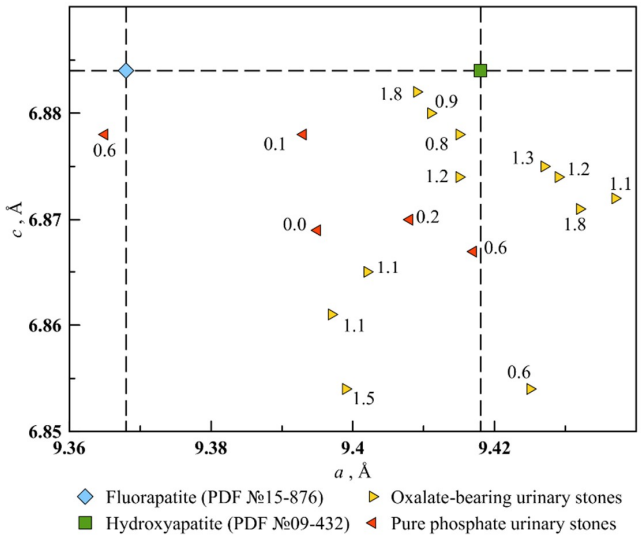

Figure 7. Unit cell parameters of the apatites formed in humans.

Fluorine is one of the components that is present in human urine, and which can not only substitute OH^- groups in hydroxylapatite, but may also influence the formation of other mineral phases, like calcium oxalates.

The results of microprobe analysis showed that the fluorine determined in the kidney stones was arranged in the apatite zones of the kidney stones. The maximum average fluorine content in the oxalate kidney stones was 1.84 wt% that was comparable with fluorapatite, for which the F content ranged from 2.1 to 3.8 wt% [26].

There was no direct correlation between the fluorine content in the studied apatites and the value of the *a* unit cell parameter (Figure 8), but at the level of a tendency we saw that the fluorine content increased with the increase of the *a* parameter. The observed increase of a unit cell parameter with the increase of fluorine content could be caused by multiple substitution mechanisms that affect unit cell parameters in different ways, since kidney stones are formed in multicomponent solutions that contain different cations and anions, which leads to different variations of the unit cell parameters. For instance, since we assume that the formation of fluorine-bearing apatite occurs in solutions with an acidic pH value, one of the most likely mechanisms is the increase in the H_2O content in the structure of apatite, which in turn significantly increases a unit cell parameter [15].

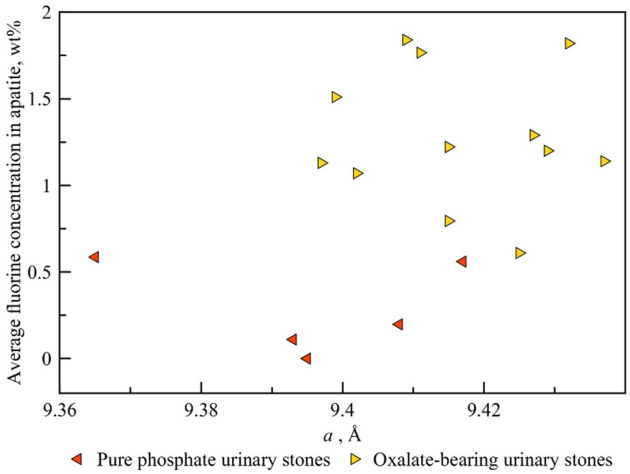

Figure 8. The plot of the *a* unit cell parameter values of the kidney stones' apatite versus its fluorine content (wt%).

4.2. Correlation between the Fluorine Content and the Amount of Oxalate Mineral Phases in a Kidney Stone

The results of the microprobe analysis rather unexpectedly showed that fluorine was present in trace amounts in the apatite of the "pure phosphate" kidney stones, while in the apatite of the oxalate-bearing stones its content was significantly higher (Table 2), which leads to a direct correlation between the content of fluorine and the amount of oxalate mineral phases in kidney stone (Figure 9). This correlation is not strict for two reasons. First of all, the process of stone formation is non-stationary, since the conditions of the medium are constantly changing, as it can be seen in Figures 2–5. The processes occurring during kidney stone nucleation can be leveled out by a sharp change in the formation conditions, because growth processes can take a very long time, for instance, more than one year. The second reason is the uneven distribution of apatite grains along the profile of the stone, so when forming the thin section, the full picture might not be obtained. An interesting fact is that the concentration of fluorine is higher in the center of the stone, which once again confirms the possibility of fluorapatite to be the nucleus of an oxalate stone formation.

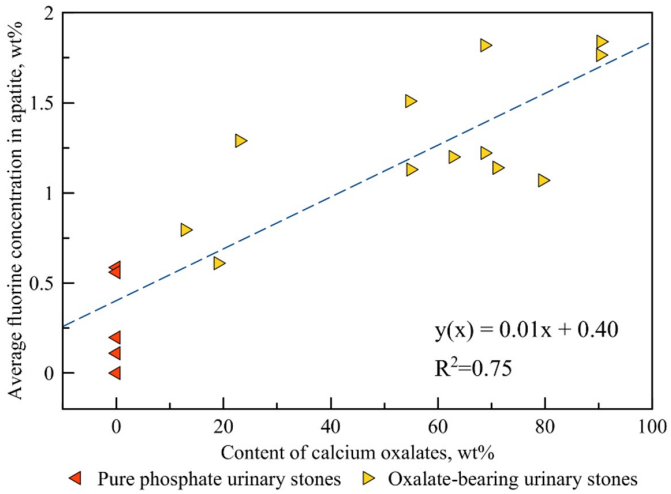

Figure 9. Direct correlation between the amount of oxalate mineral phases (wt%) and the fluorine content (wt%) in the stone.

4.3. The Effect of pH on the Thermodynamic Stability of Fluorapatite

Fluorapatite is known to be less soluble compared to hydroxylapatite [27,28]. According to the diagram (Figure 6), at the same concentration of Ca^{2+} ions fluorapatite crystallizes in the region of lower pH values than hydroxylapatite. For example, it can be seen (pink region in Figure 6) that for a Ca^{2+} ion concentration of 5.5 mol/L (which corresponds to the average concentration in the urine of a healthy person [21,22]) the region of crystallization of fluorapatite already starts at a pH of 3.7, while hydroxylapatite forms at a given concentration of Ca^{2+} and only at a pH larger than 7.0. This result is of great importance in understanding the role of fluorapatite in the crystallization of calcium oxalates, since it is known that the formation of calcium oxalates occurs at acidic pH values of the urine (4.5–6.5) [29]. Experimental modeling of the main oxalate phases formation formed in the human body (whewellite and weddellite) shows that calcium oxalate monohydrate forms at pH values of 5.00–6.00, and dihydrate at 4.00–5.00 [29,30]. At the same time, it is known that hydroxylapatite does not form under such acidic conditions, since its crystallization occurs only at pH 6.4–8.0 [29]. This does not allow us to explain the widely known and experimentally confirmed hypothesis about the role of apatite as a nucleus in the crystallization of calcium oxalates [7,14]. The results of the current research show that the role of the nucleus in the crystallization of oxalates can be played by fluorine-bearing apatite, the formation of which is possible at lower pH values.

5. Conclusions

The results of this study showed that the range of fluorine content in human oxalate kidney stones is quite wide and can reach 1.84 wt%, which is comparable with fluorapatite, for which the F content ranges from 2.1 to 3.8 wt% [26]. Direct correlation between the amount of oxalate mineral phases and the fluorine content was observed. At the same time, the fluorine content increases with the increase of *a* unit cell parameter, which is probably associated with a simultaneous increase in the amount of H_2O in the structure of apatite. The results of the thermodynamic modeling showed that the formation of fluorine-bearing apatite was possible at lower pH values than for hydroxylapatite, and therefore fluorapatite is a more suitable precursor for the crystallization of the calcium oxalates of kidney stones. The obtained results expand our knowledge on the chemical composition of kidney stones and the mechanisms of their formation, which contributes to a directed search for new approaches to prevent stone formation in the human urinary system.

Author Contributions: Conceptualization, A.V.K., A.R.I. and O.V.F.-K.; methodology, A.V.K. and A.R.I.; investigation, A.V.K. and A.R.I.; writing—original draft preparation, A.V.K. and A.R.I.; writing—review and editing, A.V.K., A.R.I. and O.V.F.-K.; visualization, A.V.K. and A.R.I. All authors have read and agreed to the published version of the manuscript.

Funding: This research was funded by the Russian Science Foundation (grant 18-77-00026 to A.V.K. and A.R.I.).

Acknowledgments: The laboratory researches were carried out in the Research Park of Saint Petersburg State University: XRD measurements—in the X-ray Diffraction Centre; SEM investigations—in the Centre for Geo-Environmental Research and Modeling (Geomodel). We are grateful to reviewers for useful comments.

Conflicts of Interest: The authors declare no conflict of interest.

References

1. Shattock, S.G. A prehistoric or predynastic Egyptian calculus. *Trans. Pathol. Soc. Lond.* **1905**, *56*, 275–290.
2. Chatterjee, P.; Chakraborty, A.; Mukherjee, A.K. Phase composition and morphological characterization of human kidney stones using IR spectroscopy, scanning electron microscopy and X-ray Rietveld analysis. *Spectrochim. Acta Part A Mol. Biomol. Spectrosc.* **2018**, *200*, 33–42. [CrossRef] [PubMed]
3. Chou, Y.-H.; Li, C.-C.; Hsu, H.; Chang, W.-C.; Liu, C.-C.; Li, W.-M.; Ke, H.-L.; Lee, M.-H.; Liu, M.-E.; Pan, S.-C.; et al. Renal function in patients with urinary stones of varying compositions. *Kaohsiung J. Med Sci.* **2011**, *27*, 264–267. [CrossRef] [PubMed]
4. Golovanova, O.A.; Punin Yu, O.; Izatulina, A.R.; Yelnikov, V.Y.; Plotkina Yu, V. Structural-tex-tural features and ontogenetic regularities of renal stone formation. *Vestn. St. Peterbg. Univ. Seriya Geol. I Geogr.* **2009**, *1*, 26–34. (In Russian)
5. Otnes, B. Correlation Between Causes and Composition of Urinary Stones. *Scand. J. Urol. Nephrol.* **1983**, *17*, 93–98. [CrossRef] [PubMed]
6. Evan, A.P. Physiopathology and etiology of stone formation in the kidney and the urinary tract. *Pediatr. Nephrol.* **2010**, *25*, 831–841. [CrossRef] [PubMed]
7. Tiselius, H.; Lindbäck, B.; Fornander, A.; Nilsson, M. Studies on the role of calcium phosphate in the process of calcium oxalate crystal formation. *Urol. Res.* **2009**, *37*, 181–192. [CrossRef] [PubMed]
8. Randall, A. The etiology of primary renal calculus. *Int. Abstr. Surg.* **1940**, *71*, 209–240.
9. Evan, A.P.; Lingeman, J.E.; Coe, F.L.; Parks, J.H.; Bledsoe, S.B.; Shao, Y.; Sommer, A.J.; Paterson, R.F.; Kuo, R.L.; Grynpas, M. Randall's plaque of patients with nephrolithiasis begins in basement membranes of thin loops of Henle. *J. Clin. Investig.* **2003**, *111*, 607–614. [CrossRef] [PubMed]
10. Sethmann, I.; Wendt-Nordahl, G.; Knoll, T.; Enzmann, F.; Simon, L.; Kleebe, H.-J. Microstructures of Randall's plaques and their interfaces with calcium oxalate monohydrate kidney stones reflect underlying mineral precipitation mechanisms. *Urolithiasis* **2017**, *45*, 235–248. [CrossRef] [PubMed]
11. Tiselius, H. Hypothesis of calcium stone formation: An interpretation of stone research during the past decades. *Urol. Res.* **2011**, *39*, 231–243. [CrossRef] [PubMed]
12. El'nikov, V.Y.; Rosseeva, E.V.; Golovanova, O.A.; Frank-Kamenetskaya, O.V. Thermodynamic and Experimental Modeling of the Formation of Major Mineral Phases of Uroliths. *Russ. J. Inorg. Chem.* **2007**, *52*, 150–157.
13. Izatulina, A.R.; Yelnikov, V. Structure, chemistry and crystallization conditions of calcium oxalates—The main components of kidney stones. In *Minerals as Advanced Materials I*; Krivovichev, S., Ed.; Springer: Berlin, Germany, 2008; pp. 231–241.
14. Xie, B.; Halter, T.J.; Borah, B.M.; Nancollas, G.H. Aggregation of calcium phosphate and oxalate phases in the formation of renal stones. *Cryst. Growth Des.* **2014**, *15*, 3038–3045. [CrossRef] [PubMed]
15. Frank-Kamenetskaya, O.V.; Izatulina, A.R.; Kuz'mina, M.A. Ion substitutions, non-stoichiometry, and formation conditions of oxalate and phosphate minerals of the human. In *Biogenic-Abiogenic Interactions in Natural and Anthropogenic Systems*; Frank-Kamenetskaya, O.V., Panova, E.G., Vlasov, D.Y., Eds.; Springer: Cham, Switzerland, 2016; pp. 425–442.
16. Frank-Kamenetskaya, O.V. Crystal chemistry and synthesis of carbonate apatites—Main minerals in living organisms. In Proceedings of the 9th International Congress for Applied Mineralogy, Brisbane, Australia, 8–10 September 2008; Australasian Institute of Mining and Metallurgy: Carlton, Australia, 2008.

17. *Topas V4.2: General Profile and Structure Analysis Software for Powder Diffraction Data*; Bruker AXS: Karlsruhe, Germany, 2009.
18. Robie, R.A.; Hemingway, B.S.; Fisher, J.R. *Thermodynamic Properties of Minerals and Related Substances at 298.15 K and 1 bar (105 Pascals) Pressure and at Higher Temperatures*, 2nd ed.; United States Government Printing Office: Washington, DC, USA, 1979; 464p.
19. Naumov, G.B.; Ryzhenko, B.N.; Khodakovsky, I.L. *Handbook of Thermodynamic Quantities (for Geologists)*, 1st ed.; Atomizdat: Moscow, Russia, 1971; 240p. (In Russian)
20. Tušl, J. Direct determination of fluoride in human urine using the fluoride electrode. *Clin. Chim. Acta* **1970**, *27*, 216–218. [CrossRef]
21. Borodin, E.A. *Biochemical Diagnosis*; V. 1,2; Amuruprpoligraphizdat: Blagoveschensk, Russia, 1989; p. 77. (In Russian)
22. Moskalev, Y.I. *Mineral Exchange*; Medicine: Moscow, Russia, 1985; p. 288. (In Russian)
23. Izatulina, A.R.; Gurzhiy, V.V.; Krzhizhanovskaya, M.G.; Chukanov, N.V.; Panikorovskii, T.L. Thermal Behavior and Phase Transition of Uric Acid and Its Dihydrate Form, the Common Biominerals Uricite and Tinnunculite. *Minerals* **2019**, *9*, 373. [CrossRef]
24. Izatulina, A.R.; Punin, Y.O.; Golovanova, O.A. To the formation of aggregate structures of kidney stones. *J. Struct. Chem.* **2014**, *55*, 1225–1231. [CrossRef]
25. Brown, P.W.; Constantz, B. *Hydroxyapatite and Related Materials*; CRC: Boca Raton, FL, USA, 1994; 368p.
26. Hovis, G.L.; Scott, B.T.; Altomare, C.M.; Leaman, A.R.; Morris, M.D.; Tomaino, G.P.; McCubbin, F.M. Thermal expansion of fluorapatite-hydroxylapatite crystalline solutions. *Am. Mineral.* **2014**, *99*, 2171–2175. [CrossRef]
27. Driessens, F.C.M. Relation between apatite solubility and anti-cariogenic effect of fluoride. *Nature* **1973**, *243*, 420–421. [CrossRef] [PubMed]
28. Moreno, E.C.; Kresak, M.; Zahradnik, R.T. Fluoridated hydroxyapatite solubility and caries formation. *Nature* **1974**, *247*, 64–65. [CrossRef] [PubMed]
29. Kuz'mina, M.A.; Nikolaev, A.M.; Frank-Kamenetskaya, O.V. The formation of calcium and magnesium phosphates of the renal stones depending on the composition of the crystallization medium. In *Processes and Phenomena on the Boundary between Biogenic and Abiogenic Nature*; Frank-Kamenetskaya, O.V., Vlasov, D.Y., Panova, E.G., Lessovaia, S.N., Eds.; Springer: Cham, Switzerland, 2019; pp. 107–118.
30. Bretherton, T.; Rodgers, A. Crystallization of calcium oxalate in minimally diluted urine. *J. Cryst. Growth* **1998**, *192*, 448–455. [CrossRef]